

Novel Sterically Hindered Substituted Ferrocenes and Their Transition Metal Complexes

Charlotte K. A. Gregson, Nicholas J. Long,* Andrew J. P. White, and David J. Williams

Department of Chemistry, Imperial College London, South Kensington, London, SW7 2AZ U.K.

Received March 30, 2004

Bis(1'-organylthiolatoferrocenylene)disulfanes, RS-fc-SS-fc-SR type **I** ligands (R = Me, ^tBu), have been synthesized by cleavage of 1,2,3-trithia[3]ferrocenophane with organolithium reagents, RLi. The disulfanes have been successfully cleaved using lithium triethylborohydride and then reacted with dibromo-organyl species (Br-X-Br) to produce a novel series of sterically hindered ligands, RS-fc-S-X-S-fc-SR type **II** ligands {(1) R = ^tBu; X = CH₂CH₂-CH₂, CH₂C₅H₃NCH₂, CH₂C₁₀H₆CH₂; (2) R = Me; X = CH₂CH₂CH₂, CH₂C₅H₃NCH₂, CH₂C₁₀H₆-CH₂}. Both type **I** and type **II** ligands have been structurally characterized, and their coordination chemistry has been investigated by reaction with the late transition metal reagents Cu(MeCN)₄PF₆ and Pd(cod)Cl₂. The resulting Cu(I) and Pd(II) complexes have been fully characterized, showing some unusual reactivity and a preponderance for a bis-bidentate chelating mode.

Introduction

The use of bulky ligands to stabilize low coordination numbers in metal complexes, and to stabilize highly reactive centers by shielding them from reaction, is now well developed.¹ In general such effects are related purely to the steric bulk of the ligands, with most examples cited in the literature being based on carbon and the heteroatoms silicon, nitrogen, and phosphorus, together with some sulfur-containing ligands, their related metal complexes, and associated catalytic applications. The utilization of bulky ligands in organometallic chemistry is a proven means to compounds that would normally be regarded as unstable. This practice has achieved great prominence in the organometallic chemistry of the heavier group 13 elements with aryl ligands.^{2,3} The major set of carbon-containing bulky ligands are those based on the cyclopentadienyl ligand (η -C₅H₅). The importance of this ligand is primarily due to the ease of synthesis of complexes incorporating one or more cyclopentadienyl rings.^{4,5}

Much novel chemistry has also emerged from studies of compounds in which a bulky tris(trimethylsilyl)methyl ligand (Me₃Si)₃C (R*) (the 'trisyl' ligand) or a closely related species (PhMe₂Si)₃C (R**) hinders nucleophilic attack at functional centers. Other unusual reactions appear to arise from the relief of steric strain

in more crowded compounds.^{6–9} Bulky alkyl ligands functionalized with N-donor groups have been employed in the stabilization of organometallic species with unusual bonding configurations.¹⁰ The properties of bulky N-containing ligands may also be tailored in order to obtain appealing chemistry.¹¹ N-Donor ligands have also been employed in cyclopentadienyl chemistry, i.e., in substituted ferrocenyleneamines.¹² Furthermore, nitrogen-based sterically demanding ligands have found application in Ni(II) diimine-catalyzed olefin polymerizations¹³ and as epoxidation catalysts.¹⁴ Sterically demanding phosphine ligands of type PR₃ influence both the lability (inertness) and coordination numbers of complexes that they are bound to; a variety of work has

(6) Eaborn, C.; Smith, J. D. *Coord. Chem. Rev.* **1996**, *154*, 125.

(7) Eaborn, C. *J. Chem. Soc., Dalton Trans.* **2001**, 3397.

(8) For a more comprehensive review of the preparation of compounds containing the R*, R**, and other related ligands attached to metals and metalloids, see: Lickiss, P. D. In *Organic Functional Group Transformations*; Pergamon: Oxford, 1995; Vol. 6, Section 6.13.2.2.

(9) (a) Cary, D. R.; Arnold, J. *Inorg. Chem.* **1994**, *33*, 1791. (b) Cary, D. R.; Ball, G. E.; Arnold, J. *J. Am. Chem. Soc.* **1995**, *117*, 3492. (c) Hawrelak, E. J.; Sata, D.; Ladipo, F. T. *J. Organomet. Chem.* **2001**, *620*, 127. (d) Al-Juaid, S. S.; Eaborn, C.; El-Hamruni, S. M.; Hitchcock, P. B.; Smith, J. D.; Sözerli, S. E. *Can. J. Organomet. Chem.* **2002**, *649* (2), 121–7.

(10) Andrews, P. C.; Raston, C. L. *J. Organomet. Chem.* **2000**, *600*, 174.

(11) (a) Clegg, W.; Drummond, A. M.; Mulvey, R. E.; O'Shaughnessy, P. *Chem. Commun.* **1997**, 1301. (b) Reger, D. L.; Wright, T. D.; Smith, M. D. *Inorg. Chim. Acta* **2002**, *334*, 1. (c) Otter, C. A.; Bardwell, D. A.; Couchman, S. M.; Jeffery, J. C.; Maher, J. P.; Ward, M. D. *Polyhedron* **1998**, *17*, 211.

(12) (a) Shafir, A.; Power, M. P.; Whitener, G. D.; Arnold, J. *Organometallics*, **2000**, *19*, 3978. (b) Gibson, V. C.; Long, N. J.; Marshall, E. L.; Oxford, P. J.; White, A. J. P.; Williams, D. J. *J. Chem. Soc., Dalton Trans.* **2001**, 1162. (c) Gibson, V. C.; Halliwell, C.; Long, N. J.; Oxford, P. J.; Smith, A. M.; White, A. J. P.; Williams, D. J. *J. Chem. Soc., Dalton Trans.* **2003**, 918.

(13) (a) Cotton, F. A.; Hong, B. *Prog. Inorg. Chem.* **1992**, *40*, 179. (b) Deng, L.; Woo, T. K.; Cavallo, L.; Margl, P. M.; Ziegler, T. *J. Am. Chem. Soc.* **1997**, *119*, 6177. (c) Britovsek, G. J. P.; Gibson, V. C.; Wass, D. F. *Angew. Chem., Int. Ed.* **1999**, *38*, 428.

(14) Chen, J.; Woo, L. K. *J. Organomet. Chem.* **2000**, *601*, 57.

* Corresponding author. Tel: +44 020 7594 5781. Fax: +44 020 7594 5804. E-mail: n.long@imperial.ac.uk.

(1) Gerloch, M.; Constable, E. C. *Transition Metal Chemistry*; VCH: Weinheim, 1994.

(2) Su, J.; Li, X.; Robinson, G. H. *Chem. Commun.* **1998**, 2015.

(3) (a) Jerius, J. J.; Hahn, J. M.; Rahman, A. F. M. M.; Mols, O.; Isley, W. H.; Oliver, J. P. *Organometallics* **1986**, *5*, 1812. (b) Beachley, O. T.; Churchill, M. R.; Pazik, J. C.; Ziller, J. W. *Organometallics* **1986**, *5*, 1814.

(4) Batsanov, A. S.; Bridgewater, B. M.; Howard, J. A. K.; Hughes, A. K.; Wilson, C. *J. Organomet. Chem.* **1999**, *590*, 169.

(5) Long, N. J.; Martin, A. J.; Vilar, R.; White, A. J. P.; Williams, D. J.; Younus, M. *Organometallics* **1999**, *18*, 4261.

been undertaken in this area with a view to designing asymmetric multidentate ligands, particularly in relation to the phenomenon of hemilability.¹⁵ The use of ferrocenylene phosphines as ligands in coordination chemistry is also well documented¹⁶ and is indeed dominated by dppf [1,1'-bis(diphenylphosphino)ferrocene], whose complexes have found catalytic application in a range of coupling¹⁷ and hydrogenation reactions.¹⁸

The extreme versatility of sulfur-containing ligands in organometallic complexes has been widely established,¹⁹ and in analogy to dppf there also exist a number of sulfur-based 1,1'-disubstituted ligands.²⁰ Following on from work in this laboratory relating to sterically hindered ligands of type RS-fc-SS-fc-SR²¹ and considering that, in comparison to other heteroatoms, work relating to sulfur has been relatively unexplored in this area, we decided to target sulfur-containing ferrocene ligands that would demonstrate a range of steric hindrance and investigate their possible coordination chemistry with appropriate transition metals, with a view to catalytic applications.

Results and Discussion

Type I Ligands. Type I ligands are the necessary precursors for the type II ligands and may be prepared by existing methods.^{20c,22} 1,2,3-Trithia[3]ferrocenophane reacts with organolithium compounds, RLi, to form bis-(1'-organylthiolatoferrocenylene)disulfanes, RS-fc-SS-fc-SR (R = Me, ^tBu²¹) type I ligands, after air oxidation (Figure 1). Exposing the reaction to air is essential to obtain pure products. Possible side-products also include species such as RSS-fc-SS-fc-SSR and RSS-fc-SS-fc-SR, which may be separated from the desired product by column chromatography (hexane/DCM, 7:3). This reaction is limited only by the available organolithium species and may therefore include a diverse range of species. The methyl derivative (**1**) was isolated as a dark orange-brown oil, which solidified on standing, while the *tert*-butyl (**2**) derivative was obtained as a yellow-gold solid.

¹H NMR spectroscopy of the ferrocenylene region of 1,1'-symmetrically sulfur-substituted ferrocenes, i.e.,

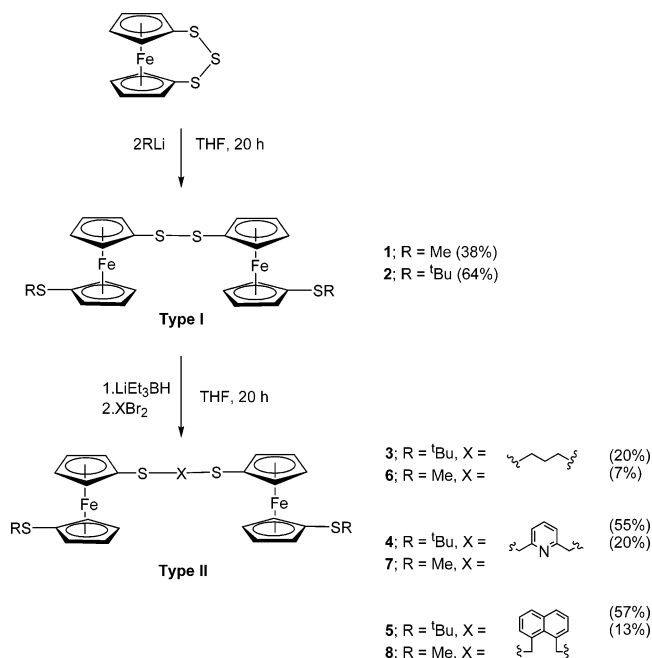


Figure 1. Formation of type I (**1** and **2**) and type II (**3–8**) ligands.

1,2,3-trithia[3]ferrocenophane, shows four multiplet signals from each of the four inequivalent cyclopentadienyl protons.²³ A similar pattern would be expected for **1** and **2**, except that the two cyclopentadienyl rings are now inequivalent due to the different substituents on each of the rings. This further complicates the spectrum, and substantial deviations are seen from the 1,2,3-trithia[3]ferrocenophane splitting pattern. Assignments were made on the basis of integral values that corresponded to expected numbers of protons present. Common to all is the high-field pseudo-triplet. For **1**, the other three triplets extensively overlap, producing a complicated but well-resolved multiplet. For **2** however, another triplet is observed along with a broad singlet. The positive FAB mass spectra show molecular ions and peaks from the symmetrical cleavage of the disulfide bridges.

Type II Ligands. To introduce bridging species between the two linked sulfurs in the type I ligands and increase the steric bulk of the ligand as well as its coordination possibilities, the disulfide bond was cleaved using organolithium reagents or, in this case, LiEt₃BH. This method has already been successfully performed in the case of bis(1'-mesitylthiolatoferrocenylene)disulfane, to give a monoferrocenediyl species.^{20c} The sulfur anions were then reacted with a selection of dibromo species (Figure 1). Column chromatography (hexane/DCM) enabled separation of the products from starting materials and other byproducts. Yields of the desired products were improved by refluxing the mixture for 3 h on addition of the superhydride and also after the 20 h overnight stirring period. The novel ligands **3–5** were all isolated as yellow solids, while **6–8** were isolated as yellow-brown oils. All gave good

(15) (a) Bader, A.; Lindner, E. *Coord. Chem. Rev.* **1991**, *108*, 27. (b) Dilworth, J. R.; Wheatley, N. *Coord. Chem. Rev.* **2000**, *199*, 89.

(16) Cullen, W. R.; Woollins, J. D. *Coord. Chem. Rev.* **1981**, *39*, 1.

(17) (a) Hayashi, T.; Tajika, M.; Tamao, K.; Kumada, M. *J. Am. Chem. Soc.* **1976**, *3718*. (b) Hayashi, T.; Konishi, M.; Kumada, M. *J. Organomet. Chem.* **1980**, *186*, C1. (c) Cai, D.; Payack, J. F.; Bender, D. R.; Hughes, D. L.; Verhoeven, T. R.; Reider, P. J. *J. Org. Chem.* **1994**, *59*, 7180. (d) Hartwig, J. F. *Synlett* **1997**, 329. (e) Hartwig, J. F. *Acc. Chem. Res.* **1998**, *31*, 852. (f) Colacot, T. J. *Platinum Metals Rev.* **2001**, *45*, 22.

(18) (a) Cullen, W. R.; Woollins, J. D. *Can. J. Chem.* **1982**, *60*, 1793. (b) Cullen, W. R.; Kim, T.-J.; Einstein, F. W. B.; Jones, T. *Organometallics* **1985**, *4*, 346. (c) Butler, I. R.; Cullen, W. R.; Kim, T.-J.; Rettig, S. J.; Trotter, J. *Organometallics* **1985**, *4*, 972.

(19) Vergamini, P. J.; Kubas, G. J. *Prog. Inorg. Chem.* **1976**, *21*, 261.

(20) (a) Long, N. J. *Metallocenes: An Introduction to Sandwich Complexes*; Blackwell Science: Oxford, 1998. (b) Gibson, V. C.; Long, N. J.; White, A. J. P.; Williams, C. K.; Williams, D. J. *Organometallics* **2000**, *19*, 4425. (c) Gibson, V. C.; Long, N. J.; White, A. J. P.; Williams, C. K.; Williams, D. J. *Chem. Commun.* **2000**, 2359. (d) Gibson, V. C.; Long, N. J.; White, A. J. P.; Williams, C. K.; Williams, D. J. *Organometallics* **2002**, *21*, 770.

(21) Gibson, V. C.; Long, N. J.; Long, R. J.; White, A. J. P.; Williams, C. K.; Williams, D. J.; Grigiotti, E.; Zanello, P. *Organometallics* **2004**, *23*, 957.

(22) Herberhold, M.; Brendel, H.-D. *J. Organomet. Chem.* **1991**, *413*, 65.

(23) (a) Barr, T. H.; Watts, W. E. *Tetrahedron* **1968**, *24*, 6111. (b) Bishop, J. J.; Davidson, A.; Katcher, M. L.; Lichtenberg, D. W.; Merrill, R. E.; Smart, J. C. *J. Organomet. Chem.* **1971**, *27*, 241. (c) Davidson, A.; Smart, J. C. *J. Organomet. Chem.* **1979**, *174*, 321. (d) Abel, E. W.; Booth, M.; Orrell, K. G. *J. Organomet. Chem.* **1981**, *208*, 213. (e) Ushijima, H. *Bull. Chem. Soc. Jpn.* **1990**, *63*, 1015.

solubility in nonpolar and polar solvents. The linking groups (X) were chosen to cover as diverse a range of species as possible, from alkyl to aromatic moieties as well as the inclusion of extra heteroatoms, to see if this had any effect on the chemistry of the ligands, particularly with regard to the type of metal complexes that would form. [In the case of **3** and **6**, the dibromo species 1,3-dibromopropane was purchased from Aldrich. For the other dibromo species, 2,6-dibromolutidine²⁴ was prepared with slight modifications to literature procedures, while 1,8-dibromomethylnaphthalene²⁵ was synthesized by a standard literature preparation.]

As with the bis(1'-organylthiolatofero-cenylene)-disulfanes (type **I** ligands), a AA'BB'CC'DD' splitting pattern is expected in the ¹H NMR spectra, with four pseudotriplets arising from the inequivalence of the two cyclopentadienyl rings. In general for **3–5** (R = ^tBu) this pattern is observed, although there is significant overlapping and broadening in the spectra, so assigning the multiplets to specific protons is therefore difficult. It is interesting to note that the shifts fall in the same region as those observed for the dimer starting material **2**, indicating that the nature of the group X has no significant effect either sterically or electronically on the protons on the cyclopentadienyl ring. **3** shows a broadened pseudotriplet, while **4** and **5** show more resolved pseudo triplets, with overlapping occurring in both cases. Each of the compounds **3–5** have distinct regions in their ¹H NMR spectra that characterize their X linking groups. Compared to the dibromide species, the X values for the type **II** ligands are all shifted upfield by between 0.2 and 0.8 ppm, indicating greater shielding due to the steric bulk of the compounds formed. For **3**, the propane unit gives two signals, one from the central CH₂ coupling to the outer four protons to give a quintet and the other from the four outer protons coupling to the central two to give a triplet. In the case of **4** and **5**, the CH₂ units are significantly further downfield than the CH₂ groups of propane, due to anisotropic deshielding effects of the aromatic pyridine and naphthalene moieties. In the case of the pyridine unit in **4**, two of the three protons on the ring are equivalent and so couple to the central one to give a doublet. This central proton in turn couples to the other two to give a triplet. Further splitting patterns are seen in the case of **5**, where there are three different proton environments, which couple to each other to give the observed double doublets. The positive FAB mass spectra of **3**, **4**, and **5** show molecular ion peaks and peaks from the symmetrical cleavage of the S–C bonds, in the same positions as those observed in the fragmentation pattern of the original starting material type **I** *tert*-butyl (**2**) derivative.

As expected, the type **II** ligands where R = Me (**6–8**) give the same ¹H NMR patterns as their *tert*-butyl equivalents, except for the position of the R group, which occurs at the same position as in the type **I** methyl derivative (**1**). The AA'BB'CC'DD' splitting pattern again shows the four pseudotriplets, although once more overlapping of the signals has made it impossible to assign the signals to specific positions on the cyclopentadienyl ring. The pattern for **6** is less broad compared

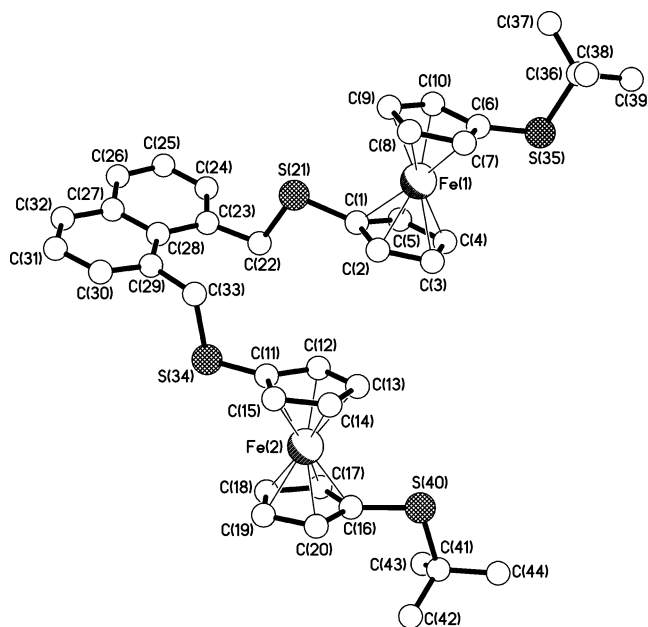


Figure 2. Molecular structure of **5**.

Table 1. Selected Bond Lengths (Å) and Angles (deg) for **5**

C(1)–S(21)	1.738(10)	C(6)–S(35)	1.741(9)
C(11)–S(34)	1.748(10)	C(16)–S(40)	1.748(9)
S(21)–C(22)	1.836(9)	C(33)–S(34)	1.833(9)
S(35)–C(36)	1.853(10)	S(40)–C(41)	1.840(12)
C(1)–S(21)–C(22)	103.9(4)	C(11)–S(34)–C(33)	99.0(4)
C(6)–S(35)–C(36)	103.5(4)	C(16)–S(40)–C(41)	103.8(4)

to **3**, while as for **4** and **5**, the patterns for **7** and **8** show overlapping of the more well-defined pseudotriplets. Similarly, the characteristic patterns resulting from the X linking groups correspond closely to those observed in the *tert*-butyl derivatives to within 0.01 ppm in most cases. Once again in the positive FAB mass spectra equivalent fragmentation patterns are seen corresponding to molecular ion peaks and fragments from cleavage at S–C bonds.

Slow evaporation of a two-layer (hexane and DCM) solution of **5** gave yellow needles. The X-ray structure determination performed on these crystals confirmed the expected structure as shown in Figure 2 (Table 1). The molecule has approximate C₂ symmetry about an axis coincident with the C(27)–C(28) bond of the naphthalene ring system. The geometries of the two ferrocenyl units are very similar, with that associated with Fe(1) being almost perfectly eclipsed (less than 1° stagger) and that for Fe(2) being staggered by only ca. 10°; in both cases their constituent Cp rings are parallel. The most noticeable departure from C₂ symmetry is in the respective orientations of the S–Cp bonds in each ferrocenyl unit. In both cases these bonds are similarly inclined [by ca. 145° for Fe(1) and by ca. 169° for Fe(2)] but having opposite signs for their S–Cp–Cp–S torsion angles. The S–Cp and S–CH₂^tBu bond lengths are in the ranges 1.738(10)–1.748(10) Å and 1.836(9)–1.853(10) Å, respectively, values comparable with those in the literature.²⁶ The only intermolecular packing interaction of note is a π -stacking of

(24) Takalo, H.; Pasanen, P.; Kankare, J. *Acta Chem. Scand., Ser. B* **1988**, *42*, 373.

(25) Szunerits, N.; Utley, J. H. P.; Nielsen, M. F. *J. Chem. Soc., Perkin Trans. 2* **2000**, 669.

(26) See for example: Zurcher, S.; Petrig, J.; Perseghini, M.; Gramlich, V.; Worle, M.; von Arx, D.; Togni, A. *Helv. Chim. Acta* **1999**, *82*, 1324.

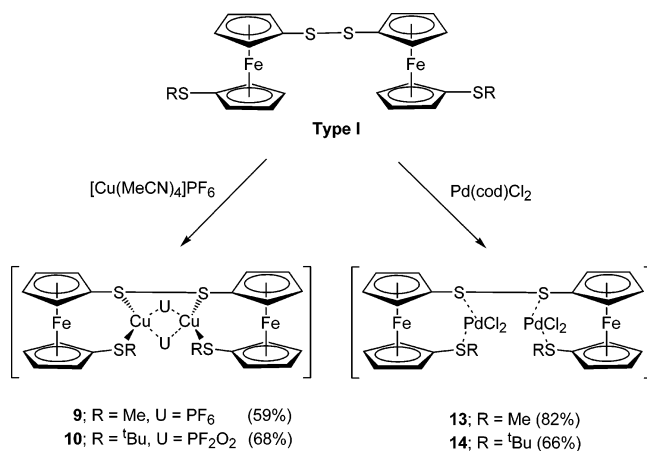


Figure 3. Formation of complexes **9**, **10**, **13**, and **14**.

the C(23)–C(28) rings of the naphthalene units in centrosymmetrically related pairs of molecules; the centroid...centroid and mean-interplanar separations are 3.88 and 3.34 Å, respectively.

Copper Complexes. Copper was chosen as the first metal to attempt to complex to the ligands, as not only has it already been extensively used to bind to sulfur-containing species¹⁵ but the tetrahedral geometry of the Cu(I) ion should have interesting consequences for the resulting metal complexes: theoretically there is the potential for the ligands to be tetradentate with respect to each copper ion, but the bulky nature of the ligands could even preclude complexation altogether.

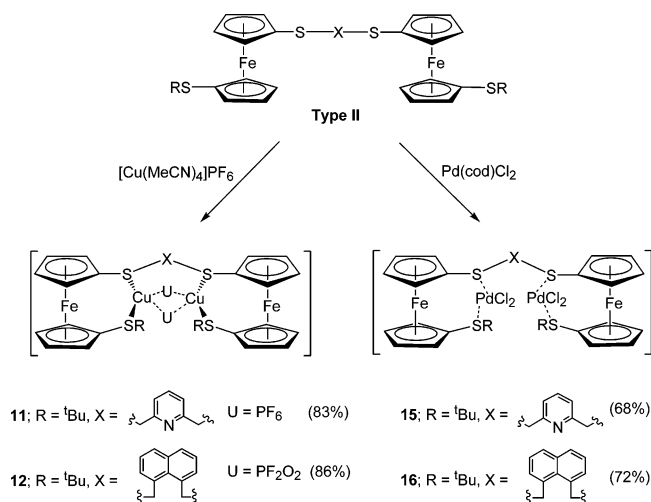


Figure 4. Formation of complexes **11**, **12**, **15**, and **16**.

The copper complexes **9**–**12** of ligands **1** and **2** (type I) (Figure 3) and **4** and **5** (type II) (Figure 4) were prepared by reacting a slight excess of the ligand with [Cu(MeCN)₄]PF₆²⁷ in DCM for 20 h at room temperature, with a darkening of the solution occurring upon reaction. After removal of the solvent in vacuo the resulting solid was washed with hexane to remove any unreacted ligand and then recrystallization was achieved from a 1:1 mixture of DCM/hexane. The complexes were all isolated as yellow-brown solids in varying yields. All of the complexes were insoluble in nonpolar solvents and only reasonably soluble in chlorinated solvents. The copper complexes give quite different spectra as com-

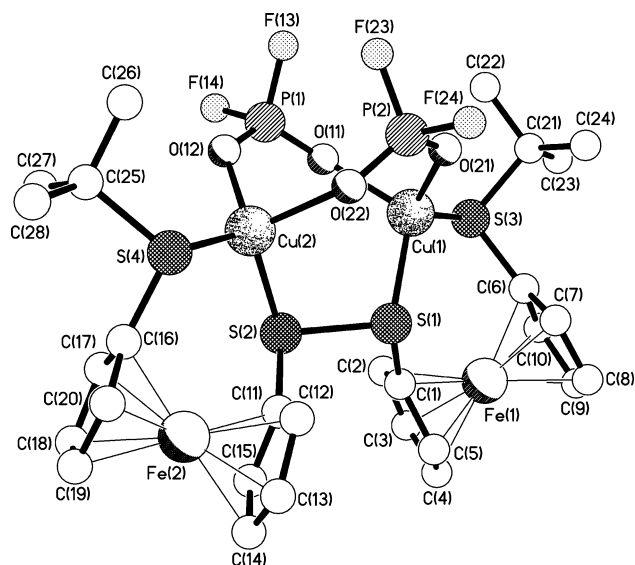


Figure 5. Molecular structure of **10**.

pared to the free uncomplexed ligands. In general all the observed peaks are now broadened, and additionally they are shifted downfield by values in the region of 0.2–0.4 ppm, indicating that all four of the sulfur atoms are binding to a copper ion in some way.

Yellow-brown needlelike crystals of **10** were obtained from a slow evaporation of a two-layer (hexane and DCM) solution. An X-ray structure determination revealed the unexpected dinuclear species illustrated in Figure 5, wherein a pair of tetrahedral, monovalent PF₂O₂ anions have been introduced into the molecule even though octahedral PF₆[−] was used in the synthesis. The molecule has approximate C₂ symmetry about an axis passing through the centers of the Cu...Cu vector and the S(1)–S(2) bond. The geometry at each copper center is distorted tetrahedral with angles in the ranges 100.3(2)–121.43(11)° at Cu(1) and 102.0(2)–118.77(13)° at Cu(2); in each case the smallest value is associated with the O–Cu–O angle. The Cu–S and Cu–O bond lengths (Table 2) are unexceptional. The angles at phosphorus in the bridging PF₂O₂ units are in the ranges 96.1(3)–122.1(3)° at P(1) and 97.4(2)–121.9(2)° at P(2), the smallest and largest angles in each case being associated with F–P–F and O–P–O, respectively. This bridging geometry is essentially the same as that observed in the complex bis(μ -2,1,6-bis(diphenylphosphino)hexane)bis(μ -2-difluorophosphate-F,O)dicopper(I).²⁸ The geometries at the four sulfur centers are distorted tetrahedral with angles at S(1) and S(2) ranging between 101.66(15)° and 110.80(15)°, and between 103.5(2)° and 114.31(16)° at S(3) and S(4). The S–Cp and S–^tBu bond lengths do not differ significantly from those observed in **5**. The S–S distance of 2.107(2) Å is ca. 0.02 Å longer than that observed in other disulfide-S,S′-dicopper(I) complexes.²⁹ Both ferrocene units have staggered geometries [ca. 21° at Fe(1) and ca. 24° at Fe(2)], and their constituent rings are inclined by between 4° and 5°; their S–Cp vectors are inclined by between 50° and 53°. There are no inter-

(28) Kitagawa, S.; Kondo, M.; Kawata, S.; Wada, S.; Maekawa, M.; Munakata, M. *Inorg. Chem.* **1995**, *34*, 1455.

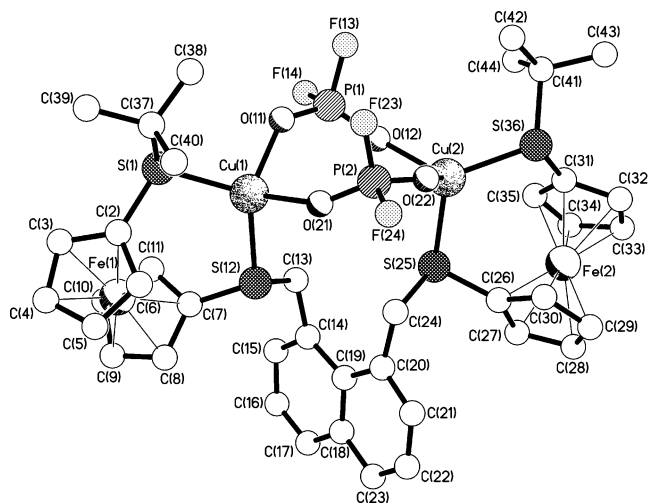
(29) For examples see: (a) Ueno, Y.; Tachi, Y.; Itoh, S. *J. Am. Chem. Soc.* **2002**, *124*, 12428. (b) Ottersen, T.; Warner, L. G.; Seff, K. *Inorg. Chem.* **1974**, *13*, 1904. (c) Ohta, T.; Tachiyama, T.; Yoshizawa, K.; Yamabe, T. *Tetrahedron Lett.* **2000**, *41*, 2581.

(27) Kubas, G. J. *Inorg. Synth.* **1990**, *28*, 68.

Table 2. Selected Bond Lengths (Å) and Angles (deg) for 10

Cu(1)–O(11)	2.078(4)	Cu(1)–O(21)	2.079(4)
Cu(1)–S(3)	2.2475(12)	Cu(1)–S(1)	2.2921(12)
Cu(2)–O(12)	2.061(4)	Cu(2)–O(22)	2.117(4)
Cu(2)–S(4)	2.2484(12)	Cu(2)–S(2)	2.2860(13)
S(1)–C(1)	1.757(5)	S(1)–S(2)	2.1065(15)
S(2)–C(11)	1.752(4)	S(3)–C(6)	1.761(5)
S(3)–C(21)	1.860(5)	S(4)–C(16)	1.755(4)
S(4)–C(25)	1.866(5)	P(1)–O(12)	1.447(4)
P(1)–O(11)	1.456(5)	P(1)–F(13)	1.514(5)
P(1)–F(14)	1.544(4)	P(2)–O(21)	1.452(4)
P(2)–O(22)	1.459(4)	P(2)–F(23)	1.531(4)
P(2)–F(24)	1.538(4)		
O(11)–Cu(1)–O(21)	100.3(2)	O(11)–Cu(1)–S(3)	102.90(14)
O(21)–Cu(1)–S(3)	121.43(11)	O(11)–Cu(1)–S(1)	115.83(16)
O(21)–Cu(1)–S(1)	105.00(13)	S(3)–Cu(1)–S(1)	111.40(5)
O(12)–Cu(2)–O(22)	102.0(2)	O(12)–Cu(2)–S(4)	118.77(13)
O(22)–Cu(2)–S(4)	102.69(12)	O(12)–Cu(2)–S(2)	109.87(14)
O(22)–Cu(2)–S(2)	108.94(13)	S(4)–Cu(2)–S(2)	113.22(4)
C(1)–S(1)–S(2)	102.12(15)	C(1)–S(1)–Cu(1)	110.80(15)
S(2)–S(1)–Cu(1)	108.50(6)	C(11)–S(2)–S(1)	101.66(15)
C(11)–S(2)–Cu(2)	109.25(15)	S(1)–S(2)–Cu(2)	105.37(6)
C(6)–S(3)–C(21)	103.5(2)	C(6)–S(3)–Cu(1)	106.69(15)
C(21)–S(3)–Cu(1)	114.31(16)	C(16)–S(4)–C(25)	103.5(2)
C(16)–S(4)–Cu(2)	108.39(14)	C(25)–S(4)–Cu(2)	114.32(17)
O(12)–P(1)–O(11)	122.1(3)	O(12)–P(1)–F(13)	109.5(3)
O(11)–P(1)–F(13)	111.4(4)	O(12)–P(1)–F(14)	108.4(3)
O(11)–P(1)–F(14)	106.0(3)	F(13)–P(1)–F(14)	96.1(3)
O(21)–P(2)–O(22)	121.9(2)	O(21)–P(2)–F(23)	108.5(3)
O(22)–P(2)–F(23)	110.4(3)	O(21)–P(2)–F(24)	107.4(3)
O(22)–P(2)–F(24)	108.3(2)	F(23)–P(2)–F(24)	97.4(2)

molecular packing interactions of note. Since the structure of **10** was not the expected product from the reaction, the starting copper complex $[\text{Cu}(\text{MeCN})_4\text{PF}_6]$ was analyzed to see if it had undergone any form of decay prior to the complexation that would explain the observed anomaly. All results, however, confirmed the presence and purity of $[\text{Cu}(\text{MeCN})_4]\text{PF}_6$. It was therefore anticipated that during the reaction and workup of **10**, some unexpected process had occurred. On consultation of the literature, it was noted that a similar phenomenon has also been found in $\{[\text{Cu}(\text{C}_9\text{H}_7\text{NS})_2](\text{PF}_2\text{O}_2)\}_2$ ³⁰ and $[\{\mu\text{-}\eta^2\text{-}\eta^2\text{-}[(\text{OC})_5\text{ReC}\equiv\text{CRe}(\text{CO})_5]\}_2\text{Cu}_4(\mu_2\text{-O}_2\text{PF}_2)_4]$.³¹ Such examples are not just confined to copper complexes however, as the first example of this phenomenon occurred with a rhodium complex, $[\{\text{Rh}(\eta^5\text{-C}_5\text{Me}_5)_2(\text{PF}_2\text{O}_2)_3]\text{PF}_6$.³² There are also occurrences with iridium, $[\{\text{Ir}(\mu\text{-SC}_6\text{H}_2\text{Me}_2\text{CH}_2)(\text{PPh}_3)(\text{XyNC})_2(\mu\text{-PF}_2\text{O}_2)]_2[\text{PF}_6]_2$;³³ ruthenium, $[\{\text{Ru}(\text{IV})(\text{POF}_3)[\text{P}(\text{OMe})_3]_2(\mu\text{-S})(\mu\text{-PF}_2\text{O}_2)_2\}]_2$;³⁴ and palladium, $[\text{Pd}(\mu\text{-PF}_2\text{O}_2)(\text{dppomf}^+)]_2$.³⁵ Although PF_6^- is usually stable, it is known to undergo hydrolysis to PF_2O_2^- and PFO_3^{2-} in the presence of various acids, aquametal complexes,³⁶ and transition metals.^{28,34,37} The oxygen source in these reactions seems to be adventitious water rather than dioxygen.³³ Matsumoto et al., on the basis of a mass spectrometry experiment using $^{18}\text{O}_2$, concluded that the oxygen atoms in the difluorophosphato ligand $[\{\text{Ru}(\text{IV})-$

**Figure 6.** Molecular structure of one (**A**) of the three independent molecules present in the crystals of **12**.

$(\text{POF}_3)[\text{P}(\text{OMe})_3]_2(\mu\text{-S})(\mu\text{-PF}_2\text{O}_2)_2]$ are derived from a trace amount of water in the solvent.³⁴ It therefore seems plausible that a similar process has occurred with **10**.

The distinction between F and O atoms, which was not conclusive with just X-ray analysis, was carried out with the aid of elemental analysis, along with ^{19}F and ^{31}P NMR spectroscopy. Results from this analysis indicated the presence of the PF_2O_2^- ion. The ^{19}F (^1H) NMR showed a broadened doublet centered at -82 ppm, $^1J = 975$ Hz, while the ^{31}P (^1H) NMR showed a triplet at -13 ppm with $^1J = 975$ Hz. It has been reported that a flapping motion of the bridging PF_2O_2^- ligand can occur,³⁴ leading to the fluorine atoms being equivalent at room temperature (rather than one axial and one equatorial), thus accounting for the broadened signal in the ^{19}F (^1H) NMR. These results indicate that for each phosphorus unit the bridging atoms are oxygen while the terminal atoms are fluorine; furthermore these values are in agreement with those found for $\text{Ir}(\text{PF}_2\text{O}_2)_2$ ³³ ($^1J_{\text{PF}} = 974$ Hz) and $\text{Ru}(\text{PF}_2\text{O}_2)_2$ ³⁴ ($^1J_{\text{PF}} = 943$ Hz).

Crystals of **12** (Figure 6) support the same bridging $\text{Cu}(\mu\text{-O}_2\text{PF}_2)_2\text{Cu}$ structure as that found for **10**, along with similar spectral splitting patterns, shifts, and coupling constants ($^1J_{\text{PF}} = 967$ Hz). It is interesting to note that ^{31}P (^1H) NMR measurements of complexes **10** and **12** immediately after washing the crude solid and before recrystallization attempts both show septets associated with the presence of the expected counteranion PF_6^- at -143 ppm, with no evidence of any other phosphorus species being present. It is therefore probable that the PF_6^- species undergoes hydrolysis during the crystallization attempts. The synthesis of **10** was in fact repeated in rigorously dried solvents, and the same X-ray structure was obtained after crystallization. The structure of **12** (Figure 6) was found to be directly analogous to that of **10**. The crystals contain three independent molecules, one of which (**A**) has approximate molecular C_2 symmetry but with disordered PF_2O_2 bridges, while the other two (**B** and **C**) both have crystallographic C_2 symmetry. The geometries at the copper centers and of the PF_2O_2 bridges do not differ markedly from those observed in **10** (Table 3). The ferrocenylene units have stagger angles of between 22° and 24° , and the $\text{S}-\text{Cp}$ and $\text{S}-\text{CH}_2^t\text{Bu}$ bond lengths do not differ significantly from those observed in **5**. In

(30) Kitagawa, S.; Kawata, S.; Nozaka, Y.; Munakata, M. *J. Chem. Soc., Dalton Trans.* **1993**, 1399.

(31) Mihan, S.; Sünkel, K.; Beck, W. *Chem. Eur. J.* **1999**, *5*, 745.

(32) White, C.; Thompson, S. J.; Maitlis, P. M. *J. Organomet. Chem.* **1977**, *134*, 319.

(33) Matsukawa, S.; Kuwata, S.; Ishii, Y.; Hidai, M. *J. Chem. Soc., Dalton Trans.* **2002**, 2737.

(34) Matsumoto, K.; Sano, Y.; Kawano, M.; Uemura, H.; Matsunami, J.; Sato, T. *Bull. Chem. Soc. Jpn.* **1997**, *70*, 1239.

(35) Gusev, O. V.; Kalsin, A. M.; Peterleitner, M. G.; Petrovskii, P. V.; Lyssenko, K. A.; Akhmedov, N. G.; Bianchini, C.; Meli, A.; Oberhauser, W. *Organometallics* **2002**, *21*, 3637.

(36) Clark, H. R.; Jones, M. M. *J. Am. Chem. Soc.* **1970**, *92*, 816.

(37) Fernández-Galán, R.; Manzano, B. R.; Otero, A.; Lanfranchi, M.; Pellinghelli, M. A. *Inorg. Chem.* **1994**, *33*, 2309.

contrast to **5** however, here there are no stacking interactions involving the naphthalene ring systems.

The copper complexes give reasonable mass spectra, with peaks evident for the presence of two copper ions and fragments from the type **I** or **II** ligand used in the complexation reactions. In the case of the unexpected structures of **10** and **12**, the observed peaks correspond to loss of PF_2O_2 rather than PF_6 as seen in the case of **9** and **11**. Elemental analysis agreed with the expected structures (featuring PF_2O_2), with no evidence of any MeCN being present.

Palladium Complexes. The palladium complexes **13–16** of ligands **1** and **2** (type **I**) (Figure 3) and **4** and **5** (type **II**) (Figure 4) have all been prepared in a fashion analogous to that for the copper complexes, by reacting a slight excess of the ligand with $[\text{Pd}(\text{cod})(\text{Cl})_2]$ ³⁸ in DCM for 20 h at room temperature. There was a darkening and color change of the solution upon reaction, and after removal of the solvent in vacuo the resulting solid was washed with hexane to remove any unreacted ligand. Recrystallization was achieved from a 1:1 mixture of DCM/hexane, and the complexes were all isolated as dark brown solids in varying yields. All of the complexes were insoluble in nonpolar solvents, and only reasonably soluble in chlorinated solvents. Palladium was chosen as the second metal to bind to the ligands, as it is known to favor sulfur-containing species,¹⁵ but also the preferred square planar geometry of the larger Pd(II) ion should have interesting consequences for the resulting metal complexes, where there is now only the potential for two bonds to form between the ligands and each palladium ion, as it is unlikely that the chloride atoms will be displaced.

As with the copper complexes, the palladium complexes also give very different NMR spectra as compared to the free uncomplexed ligands **1**, **2**, **4**, and **5**. Again all the observed peaks are now broadened, and additionally some are shifted downfield by values in the region of again around 0.3 ppm. The palladium complexes gave expected mass spectra, with peaks evident for molecular ions, loss of chloride ions with expected isotope splitting patterns,³⁹ and fragments of the free ligand. Evidence for complex formation also comes from the elemental analyses of some of the complexes, and for **16** the structure was confirmed by an X-ray diffraction study. As anticipated the ligand **5** binds to two palladium centers with each metal retaining a pair of *cis* chloride atoms (Figure 7). The geometry at the metal centers is distorted square planar with *cis* angles ranging between $80.70(5)^\circ$ and $97.20(6)^\circ$ at Pd(1) and between $83.49(5)^\circ$ and $95.14(6)^\circ$ at Pd(2), the acute angles in each case corresponding to the bite of the ferrocenylene ligand (Table 4). The Pd(1)–S(1) and Pd(2)–S(36) bond lengths of 2.325(2) and 2.329(2) Å, respectively, do not differ significantly from those seen in the related complex dichloro(1,1'-bis(isobutylthio)ferrocene)palladium (av 2.326 Å).⁴⁰ In contrast the Pd(1)–S(12) and Pd(2)–S(25) distances are anomalous at 2.2993(14) and 2.3605(14) Å, respectively; the reason for these differences is not immediately apparent. The Pd–Cl bond lengths are unexceptional. The ferrocene-

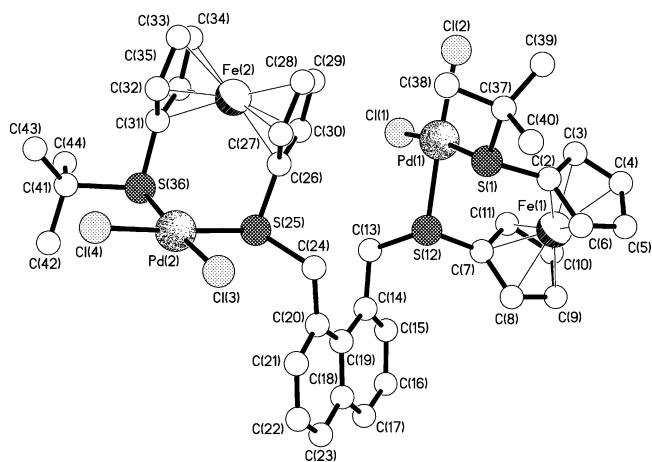


Figure 7. Molecular structure of **16**.

nylene units both have eclipsed geometries (stagger angles of ca. 1°) and parallel ring systems. The angles at S(1) and S(36) are in the ranges $100.3(2)–122.3(2)^\circ$ and $103.0(2)–122.7(2)^\circ$, and those at S(12) and S(25) lie between $101.61(19)^\circ$ and $113.09(18)^\circ$ and between $98.4(3)^\circ$ and $115.51(18)^\circ$, respectively, values in a wider range than those observed in, for example, **10**. The S–Cp and S– CH_2^tBu bond lengths do not differ significantly from those observed in the free ligand. The crystals contain both ordered and disordered solvent DCM molecules, and there are no noteworthy intermolecular interactions.

Conclusions

The main goal of this project has been achieved through the cleavage of the methyl and *tert*-butyl type **I** ligands and the incorporation of a range of linking groups to produce the novel sterically hindered substituted ferrocene type **II** ligands. The linking groups are of sufficient variety in terms of sterics and electronics to illustrate the versatility of the synthetic method. The metal bonding modes of the ligands have been investigated, and clearly a bis-bidentate binding is preferred for each ligand type, though some unusual chemistry has also been noted. Catalytic studies with metal complexes combined with electrochemical investigations will be the subject of future research.

Experimental Section

General Procedures. All preparations were carried out using standard Schlenk techniques. All solvents were distilled over standard drying agents under nitrogen directly before use, and all reactions were carried out under an atmosphere of nitrogen. Deactivated (3 wt % with water) alumina gel (neutral, grade II) was used for chromatographic separations.

All NMR spectra were recorded using a Delta upgrade on a JEOL EX270 or 400 MHz spectrometer. Chemical shifts are reported in δ (ppm) using CDCl_3 (^1H δ 7.25 ppm) as the reference solvent. Mass spectra were recorded using positive FAB methods for organometallic compounds and EI for organic compounds, on a micromass Autospec Q spectrometer. Microanalyses were carried out by Mr. S Boyer of SACS (Scientific Analysis and Consultancy Services) at the University of North London. Starting materials were prepared according to adapted literature procedures and were characterized by ^1H NMR and mass spectrometry where appropriate. All other chemicals were purchased from Aldrich Chemical Co.

(38) Drew, D.; Doyle, J. R. *Inorg. Synth.* **1990**, *28*, 346.

(39) Pavia, D. L.; Lampman, G. M.; Kriz, G. S., Jr. *Introduction to Spectroscopy*; Saunders College Publishing, 1979.

(40) McCulloch, B.; Ward, D. L.; Woollins, J. D.; Brubaker, C. H., Jr. *Organometallics* **1985**, *4*, 1425.

Table 3. Selected Bond Lengths (Å) and Angles (deg) for Molecule A and for the two C₂ Symmetric Independent Molecules B and C Present in the Crystals of 12^a

A		A			
Cu(1)–S(1)	2.2404(15)	Cu(1)–O(11)	2.111(10)		
Cu(1)–S(12)	2.2744(16)	Cu(1)–O(21)	2.097(8)		
Cu(2)–O(12)	2.105(9)	Cu(2)–O(22)	2.106(8)		
Cu(2)–S(25)	2.2891(18)	Cu(2)–S(36)	2.2566(16)		
S(1)–C(2)	1.772(5)	S(1)–C(37)	1.852(6)		
C(7)–S(12)	1.763(6)	S(12)–C(13)	1.830(6)		
C(24)–S(25)	1.845(5)	S(25)–C(26)	1.742(6)		
C(31)–S(36)	1.765(6)	S(36)–C(41)	1.855(7)		
P(1)–O(11)	1.436(9)	P(1)–O(12)	1.418(8)		
P(1)–F(13)	1.509(11)	P(1)–F(14)	1.539(13)		
P(2)–O(21)	1.429(8)	P(2)–O(22)	1.417(8)		
P(2)–F(23)	1.488(8)	P(2)–F(24)	1.539(8)		
O(21)–Cu(1)–O(11)	94.8(9)	O(21)–Cu(1)–S(1)	126.3(5)		
O(11)–Cu(1)–S(1)	103.0(4)	O(21)–Cu(1)–S(12)	95.3(5)		
O(11)–Cu(1)–S(12)	125.2(8)	S(1)–Cu(1)–S(12)	113.15(6)		
O(12)–Cu(2)–O(22)	105.2(6)	O(12)–Cu(2)–S(36)	123.0(6)		
O(22)–Cu(2)–S(36)	107.3(4)	O(12)–Cu(2)–S(25)	98.7(6)		
O(22)–Cu(2)–S(25)	107.9(6)	S(36)–Cu(2)–S(25)	113.78(6)		
C(2)–S(1)–C(37)	103.4(3)	C(2)–S(1)–Cu(1)	108.04(17)		
C(37)–S(1)–Cu(1)	113.5(2)	C(7)–S(12)–C(13)	99.8(3)		
C(7)–S(12)–Cu(1)	110.98(19)	C(13)–S(12)–Cu(1)	110.2(2)		
C(26)–S(25)–C(24)	101.2(3)	C(26)–S(25)–Cu(2)	109.2(2)		
C(24)–S(25)–Cu(2)	110.2(2)	C(31)–S(36)–C(41)	104.0(3)		
C(31)–S(36)–Cu(2)	106.8(2)	C(41)–S(36)–Cu(2)	114.7(2)		
O(12)–P(1)–O(11)	125.9(9)	O(12)–P(1)–F(13)	110.8(8)		
O(11)–P(1)–F(13)	107.2(7)	O(12)–P(1)–F(14)	107.1(7)		
O(11)–P(1)–F(14)	106.0(8)	F(13)–P(1)–F(14)	95.4(9)		
O(22)–P(2)–O(21)	123.6(7)	O(22)–P(2)–F(23)	109.3(8)		
O(21)–P(2)–F(23)	109.2(7)	O(22)–P(2)–F(24)	108.5(6)		
O(21)–P(2)–F(24)	108.2(6)	F(23)–P(2)–F(24)	94.0(6)		
B		C			
Cu(1')–S(1')	2.2469(15)	2.2591(17)	Cu(1')–O(11')	2.088(4)	2.098(5)
Cu(1')–S(12')	2.2841(16)	2.2886(18)	Cu(1')–O(12')	2.113(4)	2.102(5)
S(1')–C(2')	1.767(5)	1.760(6)	S(1')–C(37')	1.857(6)	1.849(7)
C(7')–S(12')	1.747(5)	1.750(6)	S(12')–C(13')	1.830(5)	1.836(6)
P(1')–O(11')	1.425(5)	1.450(5)	P(1')–O(12')	1.422(4)	1.425(5)
P(1')–F(13')	1.488(4)	1.500(5)	P(1')–F(14')	1.512(4)	1.534(5)
O(11')–Cu(1')–O(12')	96.9(2)	101.8(2)	O(11')–Cu(1')–S(1')	112.40(16)	105.96(16)
O(12')–Cu(1')–S(1')	120.41(15)	120.60(17)	O(11')–Cu(1')–S(12')	107.55(19)	118.11(18)
O(12')–Cu(1')–S(12')	106.44(15)	96.91(18)	S(1')–Cu(1')–S(12')	111.66(6)	113.54(7)
C(2')–S(1')–C(37')	103.9(3)	103.9(3)	C(2')–S(1')–Cu(1')	108.45(18)	106.9(2)
C(37')–S(1')–Cu(1')	113.4(2)	115.1(3)	C(7')–S(12')–C(13')	99.2(3)	100.1(3)
C(7')–S(12')–Cu(1')	112.42(19)	109.9(2)	C(13')–S(12')–Cu(1')	107.9(2)	113.1(2)
O(12')–P(1')–O(11')	122.1(3)	125.3(4)	O(12')–P(1')–F(13')	109.3(3)	111.0(4)
O(11')–P(1')–F(13')	110.7(4)	106.5(3)	O(12')–P(1')–F(14')	108.7(3)	106.6(3)
O(11')–P(1')–F(14')	106.2(3)	109.1(4)	F(13')–P(1')–F(14')	96.8(3)	93.8(4)

^a See Figures S4 and S5 in the Supporting Information for the numbering schemes.**Table 4. Selected Bond Lengths (Å) and Angles (deg) for 16**

Pd(1)–S(12)	2.2993(14)	Pd(1)–Cl(2)	2.3043(15)
Pd(1)–Cl(1)	2.3126(16)	Pd(1)–S(1)	2.3258(15)
Pd(2)–Cl(4)	2.2884(16)	Pd(2)–Cl(3)	2.2987(18)
Pd(2)–S(36)	2.3294(15)	Pd(2)–S(25)	2.3605(14)
S(1)–C(2)	1.748(6)	S(1)–C(37)	1.868(6)
C(7)–S(12)	1.764(6)	S(12)–C(13)	1.848(6)
C(24)–S(25)	1.848(6)	S(25)–C(26)	1.768(6)
C(31)–S(36)	1.756(6)	S(36)–C(41)	1.899(6)
S(12)–Pd(1)–Cl(2)	177.15(6)	S(12)–Pd(1)–Cl(1)	91.84(5)
Cl(2)–Pd(1)–Cl(1)	90.07(6)	S(12)–Pd(1)–S(1)	80.70(5)
Cl(2)–Pd(1)–S(1)	97.20(6)	Cl(1)–Pd(1)–S(1)	170.84(5)
Cl(4)–Pd(2)–Cl(3)	88.00(7)	Cl(4)–Pd(2)–S(36)	95.14(6)
Cl(3)–Pd(2)–S(36)	175.68(7)	Cl(4)–Pd(2)–S(25)	177.49(7)
Cl(3)–Pd(2)–S(25)	93.25(6)	S(36)–Pd(2)–S(25)	83.49(5)
C(2)–S(1)–C(37)	105.2(3)	C(2)–S(1)–Pd(1)	100.3(2)
C(37)–S(1)–Pd(1)	122.3(2)	C(7)–S(12)–C(13)	104.8(3)
C(7)–S(12)–Pd(1)	101.61(19)	C(13)–S(12)–Pd(1)	113.09(18)
C(26)–S(25)–C(24)	98.4(3)	C(26)–S(25)–Pd(2)	100.95(19)
C(24)–S(25)–Pd(2)	115.51(18)	C(31)–S(36)–C(41)	103.0(3)
C(31)–S(36)–Pd(2)	103.8(2)	C(41)–S(36)–Pd(2)	122.7(2)

Synthesis of Type I and Type II Ligands. Bis(1'-methylthiolatoferrocenylene)disulfane (MeS-fc-SS-fc-SMe) (1). A solution of 1,2,3-trithia[3]ferrocenophane^{23b} (2.0

g, 7.1 mmol, 1 equiv) in dry deoxygenated THF (50 mL) was cooled to –78 °C and MeLi (8.86 mL, 14.2 mmol, 2 equiv in diethyl ether) added carefully. The orange solution gradually darkened on warming to room temperature and was heated under reflux for 4 h and then overnight with stirring at room temperature for 18 h. Following exposure of the reaction to air, water (50 mL) was added to quench any excess organolithium reagent and the THF solvent removed under vacuum. The aqueous layer was extracted with DCM (10 × 50 mL), and then the combined organic layers were dried (MgSO₄) and evaporated to dryness. Gradient column chromatography (8:2 then 7:3 hexane/DCM) allowed separation of the product (second fraction) as a dark orange-brown oil, which crystallized on standing (0.70 g, 1.3 mmol, 38%). ¹H NMR (CDCl₃, 270 MHz): δ_H 2.24 (s, 6H, CH₃), 4.14 (m, 4H, C₅H₄), 4.24–4.29 (m, 12H, C₅H₄). MS (FAB +ve) *m/z*: 526 (M⁺), 263 (M – MeS-fc-S⁺). Subsequent fractions were identified as containing large proportions of Me-fc-S and the dimeric species MeS-fc-SS-fc-SMe.

Bis(1'-tert-butylthiolatoferrocenylene)disulfane (tBuS-fc-SS-fc-S^tBu) (2). This was prepared under conditions similar to those described for 1, and column chromatography (7:3 hexane/DCM) allowed separation of the product (second fraction) as a yellow-gold solid (2.09 g, 3.4 mmol, 64%). ¹H NMR (CDCl₃, 270 MHz): δ_H 1.16 (s, 18H, CH₃), 4.23 (m, 4H,

C₅H₄), 4.26–4.29 (m, 12H, C₅H₄). MS (FAB +ve) *m/z* 610 (M⁺), 305 (M – ^tBuS-fc-S⁺), 249 (M – ^tBu-S-fc-S⁺). The first fraction was identified as containing large proportions of ^tBuS-fc-SS^t-Bu.

1,2-Di(1'-tert-butylthiolato)ferrocenediylthiolato)propane (BuS-fc-S-CH₂-CH₂-CH₂-S-fc-S^tBu) (3). To a solution of bis(1'-tert-butylthiolatoferrocenylene)disulfane (2) (0.50 g, 0.8 mmol, 1 equiv) in dry deoxygenated THF (50 mL) was added 1.0 M lithium triethylborohydride (1.64 mL, 1.6 mmol, 2 equiv in THF). The yellow-orange solution was stirred for 5 h, during which time it darkened slightly. A deoxygenated solution of 1,3-dibromopropane (0.08 g, 0.4 mmol, 0.5 equiv) in THF (25 mL) was then added and the solution stirred for a further 20 h. After removing the THF in vacuo, the crude product was dissolved in DCM (50 mL) and the orange solution washed with water (50 mL). The cloudy aqueous layer was further extracted with DCM (3 × 30 mL), and the combined organic layers were dried over MgSO₄ to give a dark yellow solution, which was evaporated to dryness. The product was separated by column chromatography (7:3 hexane/DCM) to give a dark yellow oil, which crystallized on standing to give a dark yellow solid (0.11 g, 0.16 mmol, 20%). Anal. Found: C 58.64, H 6.57. Calcd for C₃₁H₄₀S₄Fe₂·0.5C₆H₁₄: C 58.71, H 6.76. ¹H NMR (CDCl₃, 270 MHz): δ_H 1.68 (q, ³J = 7.2 Hz, 2H, CH₂), 1.17 (s, 18H, CH₃), 2.59 (t, ³J = 7.2 Hz, 4H, CH₂), 4.19 (m, 4H, C₅H₄), 4.24 (m, 8H, C₅H₄), 4.28 (m, 4H, C₅H₄). MS (FAB +ve) *m/z*: 652 (M⁺) 304 (M – CH₂-CH₂-CH₂-S-fc-S^tBu⁺) 73 (M – [S-fc-S^tBu] – [fc-S^tBu]⁺).

1,2-Di(1'-tert-butylthiolato)ferrocenediylthiolato)-2,6-lutidine (BuS-fc-S-CH₂-C₅H₃N-CH₂-S-fc-S^tBu) (4). This was prepared under conditions similar to those described for 3, using 2,6-dibromolutidine.²⁴ The product was separated by gradient column chromatography (1:1 hexane/DCM then DCM) to give a yellow microcrystalline solid (0.26 g, 0.4 mmol, 55%). Anal. Found: C 58.78, H 5.89, N 1.91. Calcd for C₃₅H₄₁S₄Fe₂N: C 58.74, H 5.79, N 1.96. ¹H NMR (CDCl₃, 270 MHz): δ_H 1.16 (s, 18H, CH₃), 3.84 (s, 4H, CH₂), 4.16 (m, 4H, C₅H₄), 4.22–4.27 (m, 12H, C₅H₄), 6.90 (d, ³J = 7.7 Hz, 2H, py-H), 7.40 (t, ³J = 7.7 Hz, 1H, py-H). MS (FAB +ve) *m/z*: 716 (M⁺), 441 (M – ^tBuS-fc⁺), 304 (M – CH₂-C₅H₃N-CH₂-S-fc-S^tBu⁺).

1,2-Di(1'-tertbutylthiolato)ferrocenediylthiolato)-1,8-dimethylnaphthalene (BuS-fc-S-CH₂-C₁₀H₆-CH₂-S-fc-S^tBu) (5). This was prepared under conditions similar to those described for 3, using 1,8-di(bromomethyl)naphthalene.²⁵ The product was separated by column chromatography (7:3 hexane/DCM) to give the dark yellow product (0.36 g, 0.5 mmol, 57%). Crystals suitable for X-ray analysis were grown by a two-layer method using hexane on DCM. Anal. Found: C 62.76, H 5.76. Calcd for C₄₀H₄₄S₄Fe₂: C 62.82, H 5.76. ¹H NMR (CDCl₃, 270 MHz): δ_H 1.17 (s, 18H, CH₃), 4.13 (m, 4H, C₅H₄), 4.17 (m, 8H, C₅H₄), 4.25 (m, 4H, C₅H₄), 4.49 (s, 4H, CH₂), 7.10 (dd, ³J = 7.3 Hz, ⁴J = 1.5 Hz, 1H, nap-H), 7.24 (dd, ³J = 8.5 Hz, ³J = 7.9 Hz, 1H, nap-H), 7.70 (dd, ³J = 8.2 Hz, ⁴J = 1.5 Hz, 1H, nap-H). MS (FAB +ve) *m/z*: 764 (M⁺), 459 (M – ^tBuS-fc-S⁺), 305 (M – CH₂-C₁₀H₆-CH₂-S-fc-S^tBu⁺).

Crystal data for 5: C₄₀H₄₄S₄Fe₂, *M* = 764.69, monoclinic, *C*2/*c* (no. 15), *a* = 31.455(3) Å, *b* = 6.1504(6) Å, *c* = 39.998(3) Å, β = 107.335(7)°, *V* = 7386.6(12) Å³, *Z* = 8, *D_c* = 1.375 g cm⁻³, μ(Cu Kα) = 8.611 mm⁻¹, *T* = 293 K, yellow thin platy needles; 4888 independent measured reflections, *F*² refinement, *R*₁ = 0.068, *wR*₂ = 0.146, 2505 independent observed absorption-corrected reflections [*I*_o > 4σ(*I*_o)], 2θ_{max} = 120°, 415 parameters. CCDC 234839.

1,2-Di(1'-methylthiolato)ferrocenediylthiolato)propane (MeS-fc-S-CH₂-CH₂-CH₂-S-fc-SMe) (6). To a solution of bis(1'-methylthiolatoferrocenylene)disulfane (1) (0.26 g, 0.5 mmol, 1 equiv) dissolved in dry deoxygenated THF (50 mL) was added 1.0 M lithium triethylborohydride (1.0 mL, 1.0 mmol, 2 equiv in THF). The orange solution was heated under reflux for 3 h, during which time it darkened. A deoxygenated solution of 1,3-dibromopropane (0.02 mL, 0.24 mmol, 0.5 equiv) in THF (20 mL) was then added and the solution stirred for 18 h and then

heated under reflux for a further 3 h. Removal of the THF in vacuo yielded the crude product, an orange oil. This was then dissolved in DCM (50 mL) and washed with distilled water (50 mL). The aqueous layer was further extracted with DCM (2 × 25 mL), and the combined organic layers were dried over MgSO₄. Removal of the solvent and then gradient column chromatography (1:1 hexane/DCM, then DCM, then acetone) gave a number of fractions. The first one was identified as the monosubstituted product MeS-fc-S-CH₂-CH₂-CH₂-Br, a dark brown oil. The second fraction was unused starting material MeS-fc-S-CH₂-CH₂-CH₂-S-fc-SMe. The desired product was elucidated in trace amounts as the third fraction, a bright orange oil (0.02 g, 0.04 mmol, 7%). Anal. Found: C 52.92, H 4.99. Calcd for C₂₅H₂₈S₄Fe₂: C 52.82, H 4.97. ¹H NMR (CDCl₃, 270 MHz): δ_H 1.68 (q, ³J = 7.2 Hz, 2H, CH₂), 2.28 (s, 6H, CH₃), 2.60 (t, ³J = 7.2 Hz, 4H, CH₂), 4.14 (m, 4H, C₅H₄), 4.18 (m, 4H, C₅H₄), 4.23 (m, 4H, C₅H₄), 4.27 (m, 4H, C₅H₄). MS (FAB +ve) *m/z*: 568 (M⁺), 304 (M – MeS-fc-S⁺), 263 (M – CH₂-CH₂-CH₂-S-fc-SMe⁺).

1,2-Di(1'-methylthiolato)ferrocenediylthiolato)-2,6-lutidine (MeS-fc-S-CH₂-C₅H₃N-CH₂-S-fc-SMe) (7). This was prepared under conditions similar to those described for 6, using 2,6-dibromolutidine.²⁴ The product was separated by column chromatography (1:1 hexane/DCM) to give the dark yellow-brown product as the second fraction (0.04 g, 0.06 mmol, 20%). Anal. Found: C 55.31, H 4.61, N 2.23. Calcd for C₂₉H₂₉S₄Fe₂N: C 55.15, H 4.60, N 2.22. ¹H NMR (CDCl₃, 270 MHz): δ_H 2.26 (s, 6H, CH₃), 3.81 (m, 4H, CH₂), 4.13–4.16 (m, 4H, C₅H₄), 4.25–4.28 (m, 12H, C₅H₄), 6.90 (d, ³J = 7.79 Hz, 2H, py-H), 7.39 (m, 1H, py-H). MS (FAB +ve) *m/z*: 632 (M⁺), 89 (M – [MeS-fc-S] – [CH₂-S-fc-SMe]⁺).

1,2-Di(1-methylthiolato)ferrocenediylthiolato)-1,8-dimethylnaphthalene (MeS-fc-S-CH₂-C₁₀H₆-CH₂-S-fc-SMe) (8). This was prepared under conditions similar to those described for 6, using 1,8-di(bromomethyl)naphthalene.²⁵ The product was separated by column chromatography (7:3 hexane/DCM), which gave a number of fractions. The desired product was elucidated as the third fraction, a dark yellow-orange oil (0.04 g, 0.06 mmol, 13%). Anal. Found: C 59.94, H 4.68. Calcd for C₃₄H₃₂S₄Fe₂: C 60.00, H 4.71. ¹H NMR (CDCl₃, 270 MHz): δ_H 2.24 (s, 6H, CH₃), 4.10–4.15 (m, 8H, C₅H₄), 4.18 (m, 4H, C₅H₄), 4.23–4.29 (m, 4H, C₅H₄), 4.50 (s, 4H, CH₂), 7.11 (dd, ³J = 7.03 Hz, ⁴J = 1.24 Hz, 1H, nap-H), 7.24 (dd, ³J = 8.18 Hz, ³J = 7.18 Hz, 1H, nap-H), 7.72 (dd, ³J = 8.17 Hz, ⁴J = 1.24 Hz, 1H, nap-H). MS (FAB +ve) *m/z*: 680 (M⁺), 417 (M – MeS-fc-S⁺), 263 (M – MeS-fc-S-CH₂-C₁₀H₆-CH₂⁺).

[Bis(1'-methylthiolatoferrocenylene)disulfane]bis(copper hexafluorophosphate) [(MeS-fc-SS-fc-SMe)Cu₂-P₂F₁₂] (9). A solution of 1 (0.10 g, 0.19 mmol, 1.1 equiv) was dissolved in dry deoxygenated DCM (30 mL) under nitrogen to give an orange solution. A colorless solution of [Cu(MeCN)₄]-PF₆ (0.06 g, 0.17 mmol, 1 equiv) also dissolved in DCM (30 mL) was then added, and the reaction mixture was stirred for 24 h, during which time it turned a darker orange-brown, indicating that a reaction had occurred. The solvent was removed in vacuo, to give brown-orange crystals, which were then washed with dry deoxygenated hexane (25 mL), leaving a dark brown crystalline product (0.05 g, 0.05 mmol, 59%). Anal. Found: C 32.59, H 3.54. Calcd for C₂₂H₂₂S₄Fe₂Cu₂P₂F₁₂·C₆H₁₄: C 32.66, H 3.53. ¹H NMR (CDCl₃, 270 MHz): δ_H 2.45 (s, 6H, CH₃), 4.11–4.48 (m, 16H, C₅H₄). ³¹P(¹H) NMR (CDCl₃, 270 MHz): δ_{P(H)} –144 (sp, ¹J = 713 Hz, 2P, PF₆⁻). MS (FAB +ve) *m/z*: 652 (M – P₂F₁₂⁺), 589 (M – Cu₂P₂F₁₂⁺), 526 (M – Cu₂P₂F₁₂⁺), 263 (M – [Cu₂P₂F₁₂] – [MeS-fc-S]⁺).

[Bis(1'-tert-butylthiolatoferrocenylene)disulfane]bis(copper hexafluorophosphate) [(^tBuS-fc-SS-fc-S^tBu)Cu₂-P₂F₄O₄] (10). This was prepared under conditions similar to those described for 9, to leave a dark brown-orange crystalline product (0.19 g, 0.2 mmol, 68%). Crystals suitable for X-ray analysis were grown by a two-layer method using hexane on DCM. Anal. Found: C 35.33, H 3.47. Calcd for C₂₈H₃₄S₄Fe₂Cu₂P₂F₄O₄: C 35.78, H 3.62. ¹H NMR (CDCl₃, 270 MHz): δ_H

1.28 (s, 18H, CH₃), 4.38–4.49 (m, 16H, C₅H₄). ³¹P(H) NMR (CDCl₃, 270 MHz): δ_{P(1H)} –12.89 (t, ¹J = 975 Hz, 2P, PF₂). ¹⁹F(H) NMR (CFCl₃, 400 MHz): δ_{F(1H)} –82.26 (br d, ¹J = 975 Hz, 4F, PF₂). MS (FAB +ve) *m/z*: 839 (M – PF₂O₂⁺), 736 (M – P₂F₄O₄⁺), 673 (M – CuP₂F₄O₄⁺), 610 (M – Cu₂P₂F₄O₄⁺), 305 (M – [Cu₂P₂F₄O₄] – [t-BuS-fc-S]⁺).

Crystal data for 10: C₂₈H₃₄Cu₂F₄Fe₂O₄P₂S₄, *M* = 939.51, monoclinic, *P*2₁/*c* (no. 14), *a* = 11.3709(12) Å, *b* = 14.5159(12) Å, *c* = 21.390(2) Å, β = 94.806(8)°, *V* = 3518.1(6) Å³, *Z* = 4, *D_c* = 1.774 g cm⁻³, μ(Mo Kα) = 2.384 mm⁻¹, *T* = 293 K, orange blocks; 6151 independent measured reflections, *F*² refinement, *R*₁ = 0.041, *wR*₂ = 0.084, 4618 independent observed absorption-corrected reflections [|*F*₀| > 4σ(|*F*₀|), 2θ_{max} = 50°], 416 parameters. CCDC 234840.

[1,2-Di(1'-tert-butylthiolato)ferrocenediylthiolato]-2,6-lutidene]bis(copper hexafluorophosphate) [(^tBuS-fc-S-CH₂-C₅H₃N-CH₂-S-fc-S'^tBu)]Cu₂P₂F₁₂] (11). A solution of **4** (0.05 g, 0.07 mmol, 1.1 equiv) was dissolved under nitrogen in dry deoxygenated DCM (10 mL) to give a yellow solution. To this was added a colorless solution of [Cu(MeCN)₄]PF₆²⁷ (0.02 g, 0.06 mmol, 1 equiv) also dissolved in DCM (10 mL). The reaction mixture was stirred for 24 h, and the solvent removed in vacuo, to give a dark yellow solid. The crude product was washed with dry deoxygenated hexane (10 mL) (vigorous stirring for 20 min), and the yellow washings were removed via cannula to leave the desired dark yellow product (0.03 g, 0.03 mmol, 83%). Anal. Found: C 40.53, H 4.72, N 0.97. Calcd for C₃₅H₄₁S₄Fe₂N Cu₂P₂F₁₂·C₆H₁₄: C 40.39, H 4.56, N 1.15. ¹H NMR (CDCl₃, 270 MHz): δ_H 1.32 (s, 18H, CH₃), 4.23–4.42 (m, 20H, CH₂ and C₅H₄), 7.41 (br d, 2H, py-H), 7.77 (br t, 1H, py-H). δ_{P(1H)} (270 MHz, CDCl₃): –143 (sp, ¹J = 713 Hz, 2P, PF₆). MS (FAB +ve) *m/z*: 866 (M – CuPF₉⁺), 778 (M – CuP₂F₁₂⁺).

[1,2-Di(1'-tert-butylthiolato)ferrocenediylthiolato]-1,8-dimethylnaphthalene]bis(copper μ-difluorophosphate) [(^tBuS-fc-S-CH₂-C₁₀H₆-CH₂-S-fc-S'^tBu)]Cu₂P₂F₄O₄] (12). This was prepared under conditions similar to those described for **11**, to give a dark yellow product (0.03 g, 0.03 mmol, 86%). Crystals suitable for X-ray analysis were grown by a two-layer method using hexane on DCM. Anal. Found: C 46.66, H 4.96. Calcd for C₄₀H₄₄S₄Fe₂Cu₂P₂F₄O₄·C₆H₁₄: C 46.82, H 4.96. ¹H NMR (CDCl₃, 270 MHz): δ_H 1.34 (s, 18H, CH₃), 4.13–4.47 (m, 16H, C₅H₄), 4.98 (s, 4H, CH₂), 7.35 (br m, 1H, nap-H), 7.42 (br m, 1H, nap-H), 7.78 (br m, 1H, nap-H). ³¹P(H) NMR (CDCl₃, 270 MHz): δ_{P(1H)} (270 MHz, CDCl₃): –15.36 (t, ¹J = 967 Hz, 2P, PF₂). ¹⁹F(H) NMR (CFCl₃, 400 MHz): δ_{F(1H)} –86.13 (br d, ¹J = 967 Hz, PF₂). MS (FAB +ve) *m/z*: 993 (M – PF₂O₂⁺), 827 (M – CuP₂F₄O₄⁺), 764 (M – Cu₂P₂F₄O₄⁺), 305 (M – [Cu₂P₂F₄O₄] – [t-BuS-fc-S-CH₂-C₁₀H₆-CH₂]⁺).

Crystal data for 12: C₄₀H₄₄Cu₂F₄Fe₂O₄P₂S₄, *M* = 1093.71, monoclinic, *I*2/*a* (no. 15), *a* = 22.0029(6) Å, *b* = 24.9608(6) Å, *c* = 33.2717(12) Å, β = 97.2020(10)°, *V* = 18129.0(9) Å³, *Z* = 16 (one unique and two C₂ symmetric molecules), *D_c* = 1.603 g cm⁻³, μ(Mo Kα) = 1.863 mm⁻¹, *T* = 293 K, orange-yellow blocks; 12996 independent measured reflections, *F*² refinement, *R*₁ = 0.055, *wR*₂ = 0.151, 8520 independent observed absorption-corrected reflections [|*F*₀| > 4σ(|*F*₀|), 2θ_{max} = 47°], 1121 parameters. CCDC 234841.

[Bis(1'-methylthiolatoferrocenylene)disulfane]bis(palladium dichloride) [(MeS-fc-SS-fc-SMe)]Pd₂Cl₄] (13). A solution of **1** (0.12 g, 0.24 mmol, 1.1 equiv) was dissolved in dry deoxygenated DCM (15 mL) under nitrogen to give an orange solution. A yellow solution of Pd(cod)Cl₂³⁷ (0.06 g, 0.21 mmol, 1 equiv) also dissolved in DCM (15 mL) was then added, and the reaction mixture was stirred for 20 h, during which time it darkened, turning a dark purple-black color, indicating that a reaction had occurred. The solvent was removed in vacuo, and the crude product was then washed with dry deoxygenated hexane (25 mL) to leave a dark purple-black crystalline product (0.08 g, 0.09 mmol, 82%). Anal. Found: C

34.54, H 3.76. Calcd for C₂₂H₂₂S₄Fe₂Pd₂Cl₄·C₆H₁₄: C 34.77, H 3.75. ¹H NMR (CDCl₃, 270 MHz): δ_H 2.51 (s, 6H, CH₃), 4.15–4.50 (br s, 16H, C₅H₄). MS (FAB +ve) *m/z*: 809 (M – 2Cl⁺), 774 (M – 3Cl⁺), 667 (M – Pd – 3Cl⁺), 263 (M – [Pd₂Cl₄] – [MeS-fc-S]⁺).

[Bis(1'-tert-butylthiolatoferrocenylene)disulfane]bis(palladium dichloride) [(^tBuS-fc-SS-fc-S'^tBu)]Pd₂Cl₄] (14). This was prepared under conditions similar to those described for **13**, to give a dark red-brown crystalline product (0.04 g, 0.04 mmol, 66%). Anal. Found: C 34.83, H 3.53. Calcd for C₂₈H₃₄S₄Fe₂Pd₂Cl₄: C 34.84, H 3.53. ¹H NMR (CDCl₃, 270 MHz): δ_H 1.36 (s, 18H, CH₃), 4.15–4.55 (br s, 16H, C₅H₄). MS (FAB +ve) *m/z*: 964 (M⁺), 891 (M – 2Cl⁺), 857 (M – 3Cl⁺), 753 (M – Pd – 3Cl⁺), 610 (M – Pd₂Cl₄⁺), 305 (M – [Pd₂Cl₄] – [t-BuS-fc-S]⁺).

[1,2-Di(1'-tert-butylthiolato)ferrocenediylthiolato]-2,6-lutidene]palladium Dichloride [(^tBuS-fc-S-CH₂-C₅H₃N-CH₂-S-fc-S'^tBu)]Pd₂Cl₄] (15). A solution of **4** (0.08 g, 0.11 mmol, 1.1 equiv) was dissolved in dry deoxygenated DCM (15 mL) under nitrogen to give a yellow solution. A yellow solution of Pd(cod)Cl₂³⁷ (0.03 g, 0.12 mmol, 1 equiv) also dissolved in DCM (15 mL) was then added, and the reaction mixture was stirred for 20 h, during which time it darkened, turning a blood red color, indicating that a reaction had occurred. The solvent was removed in vacuo, and the crude product was then washed with dry deoxygenated hexane (15 mL) (vigorous stirring for 15 min) to leave a dark red-brown crystalline product (0.04 g, 0.03 mmol, 68%). Anal. Found: C 42.32, H 4.64, N 1.11. Calcd for C₃₅H₄₁S₄Fe₂NPd₂Cl₄·C₆H₁₄: C 42.58, H 4.76, N 1.21. ¹H NMR (CDCl₃, 270 MHz): δ_H 1.36 (s, 18H, CH₃), 3.84 (s, 4H, CH₂), 4.16–4.49 (br s, 16H, C₅H₄), 6.92 (br d, ³J = 5.4 Hz, 2H, py-H), 7.38 (br t, ³J = 5.4 Hz, 1H, py-H). MS (FAB +ve) *m/z*: 856 (M – Pd – 3Cl⁺), 821 (M – Pd – 4Cl⁺).

[1,2-Di(1'-tert-butylthiolato)ferrocenediylthiolato]-1,8-dimethylnaphthalene]palladium Dichloride [(^tBuS-fc-S-CH₂-C₁₀H₆-CH₂-S-fc-S'^tBu)]Pd₂Cl₄] (16). This was prepared under conditions similar to those described for **15**, to give a dark red-brown crystalline product (0.03 g, 0.03 mmol, 72%). Crystals suitable for X-ray analysis were grown by a two-layer method using hexane on DCM. Anal. Found: C 44.53, H 4.51. Calcd for C₄₀H₄₄S₄Fe₂Pd₂Cl₄·0.5C₆H₁₄: C 44.48, H 4.43. ¹H NMR (CDCl₃, 270 MHz): δ_H 1.37 (s, 18H, CH₃), 4.18–4.35 (br s, 16H, C₅H₄), 4.49 (s, 4H, CH₂), 7.10 (br dd, 1H, nap-H), 7.21 (br t, 1H, nap-H), 7.72 (br dd, 1H, nap-H). MS (FAB +ve) *m/z*: 1117 (M⁺), 942 (M – PdCl₂⁺), 907 (M – Pd – 3Cl⁺), 764 (M – Pd₂Cl₄⁺), 459 (M – [Pd₂Cl₄] – [t-BuS-fc-S]⁺).

Crystal data for 16: C₄₀H₄₄Cl₄Fe₂Pd₂S₄·3CH₂Cl₂, *M* = 1374.07, triclinic, *P*1̄ (no. 2), *a* = 11.1215(13) Å, *b* = 12.1727(11) Å, *c* = 20.592(2) Å, α = 82.119(7)°, β = 83.919(7)°, γ = 73.252(6)°, *V* = 2637.7(5) Å³, *Z* = 2, *D_c* = 1.730 g cm⁻³, μ(Mo Kα) = 1.906 mm⁻¹, *T* = 293 K, orange-red platy needles; 9267 independent measured reflections, *F*² refinement, *R*₁ = 0.047, *wR*₂ = 0.102, 6834 independent observed absorption-corrected reflections [|*F*₀| > 4σ(|*F*₀|), 2θ_{max} = 50°], 595 parameters. CCDC 234842.

Acknowledgment. We are very grateful to Johnson Matthey plc for the loan of the palladium salts and to the Department of Chemistry, Imperial College London, for undergraduate project funding. We thank Dr. Ina Dix of Bruker-Nonius AXS (Karlsruhe) for collecting the single-crystal diffraction data for compound **12**.

Supporting Information Available: Details about the X-ray crystal structures in CIF format and ORTEP diagrams for **5**, **10**, **12**, and **16**. This information is available free of charge via the Internet at <http://pubs.acs.org>.

OM049775X